

# Molecular Basis for Enantioselectivity of Lipase from *Pseudomonas cepacia* toward Primary Alcohols. Modeling, Kinetics, and Chemical Modification of Tyr29 to Increase or Decrease Enantioselectivity

W. Victor Tuomi and Romas J. Kazlauskas\*

McGill University, Department of Chemistry, 801 Sherbrooke Street West,  
Montréal, Québec H3A 2K6 Canada

Received September 1, 1998 (Revised Manuscript Received January 25, 1999)

Lipase from *Pseudomonas cepacia* (PCL) shows good enantioselectivity toward primary alcohols. An empirical rule can predict which enantiomer of a primary alcohol reacts faster, but there is no reliable strategy to increase the enantioselectivity. We used a combination of molecular modeling of lipase–transition state analogue complexes and kinetic measurements to identify the molecular basis of the enantioselectivity toward two primary alcohols: 2-methyl-3-phenyl-1-propanol, **1**, and 2-phenoxy-1-propanol, **2**. In hydrolysis of the acetate esters, PCL favors the (*S*)-enantiomer of both substrates ( $E = 16$  and  $17$ , respectively), but, due to changes in priorities of the substituents, the (*S*)-enantiomers of **1** and **2** have opposite shapes. Computer modeling of transition state analogues bound to PCL show that primary alcohols bind to PCL differently than secondary alcohols. Modeling and kinetics suggest that the enantioselectivity of PCL toward **1** comes from the binding of the methyl group at the stereocenter within a hydrophobic pocket for the fast-reacting enantiomer, but not for the slow-reacting enantiomer. On the other hand, the enantioselectivity toward **2** comes from an extra hydrogen bond between the phenoxy oxygen of the substrate to the phenolic OH of Tyr29. This hydrogen bond may slow release of the (*R*)-alcohol and thus account for the reversal of enantioselectivity. To decrease the enantioselectivity of PCL toward **2**-acetate by a factor of 2 to  $E = 8$ , we eliminated the hydrogen bond by acetylation of the tyrosyl residues with *N*-acetylimidazole. To increase the enantioselectivity of PCL toward **2**-acetate by a factor of 2 to  $E = 36$ , we increased the strength of the hydrogen bond by nitration of the tyrosyl residues with tetranitromethane. This is one of the first examples of a rationally designed modification of a lipase to increase enantioselectivity.

## Introduction

Molecular recognition is the key to current problems in chemistry and biology. Stereoselective reagents recognize correct substrate orientation in the transition state. Drug action, cell–cell recognition, and receptor target recognition all rely on molecular recognition by proteins. Stereoselective and regioselective enzyme-catalyzed reactions also rely on molecular recognition and selective stabilization of transition states by proteins. This paper focuses on the ability of a lipase from *Pseudomonas cepacia* (PCL) to distinguish between enantiomers of primary alcohols. Enantioselectivity is easier to study than diastereoselectivity or other types of selectivity because the physical properties of enantiomers are identical. Thus, enantioselectivity stems directly from molecular recognition, not from differences in solubility, reactivity, etc., which may be the case for diastereomers.

Organic chemists use lipases such as PCL to resolve enantiomers and to selectively protect and deprotect synthetic intermediates.<sup>1</sup> To guide synthetic applications, chemists often use empirical rules, which summarize the known selectivities of lipases. An empirical rule for

secondary alcohols, Figure 1, predicts which enantiomer reacts faster based on the size of the substituents at the stereocenter.<sup>2</sup> This rule implies that lipases recognize enantiomers based on the size of the substituents. Indeed, researchers have increased the enantioselectivity of a reaction by increasing the size of the large substituent.<sup>3</sup> As shown in Figure 1, this rule is only qualitative, but researchers have also more precisely defined the sizes of the medium and large substituents using either box models<sup>4</sup> or comparative molecular field analysis (CoMFA).<sup>5</sup>

X-ray crystallographers have solved the structures of more than 10 different lipases, including some containing bound transition state analogues.<sup>6</sup> These structures show an alcohol binding site with two pockets consistent with the empirical rule in Figure 1. One pocket is large, lined

(2) Kazlauskas, R. J.; Weissfloch, A. N. E.; Rappaport, A. T.; Cuccia, L. A. *J. Org. Chem.* **1991**, *56*, 2656–2665 and references therein.

(3) Scilimati, A.; Ngooi, T. K.; Sih, C. J. *Tetrahedron Lett.* **1988**, *29*, 4927–4930. Johnson, C. R.; Plè, P. A.; Adams, J. P. *J. Chem. Soc., Chem. Commun.* **1991**, 1006–1007. Goergens, U.; Schneider, M. P. *J. Chem. Soc., Chem. Commun.* **1991**, 1064–1066. *Ibid.* 1066–1068. Kim, M. J.; Choi, Y. K. *J. Org. Chem.* **1992**, *57*, 1605–1607. Gupta, A. K.; Kazlauskas, R. J. *Tetrahedron: Asymmetry* **1993**, *4*, 879–888. Rotticci, D.; Orrenius, C.; Hult, K.; Norin, T. *Tetrahedron: Asymmetry* **1997**, *8*, 359–362.

(4) *Pseudomonas fluorescens* lipase: Burgess, K.; Jennings, L. D. *J. Am. Chem. Soc.* **1991**, *113*, 6129–6139. Naemura, K.; Fukuda, R.; Konishi, M.; Hirose, K.; Tobe, Y. *J. Chem. Soc., Perkin Trans. 1* **1994**, 1253–1256. Naemura, K.; Fukuda, R.; Murata, M.; Konishi, M.; Hirose, K.; Tobe, Y. *Tetrahedron: Asymmetry* **1995**, *6*, 2385–2394.

(1) Kazlauskas, R. J.; Bornscheuer, U. T. *Biotechnology*, 2nd ed.; Kelly, D. R., Ed.; Wiley-VCH: Weinheim, 1998; Vol. 8a, pp 37–191; Faber, K. *Biotransformations in Organic Chemistry*, 3rd ed.; Springer: Berlin, 1997. Wong, C.-H.; Whitesides, G. M. *Enzymes in Synthetic Organic Chemistry*; Pergamon: New York, 1994. Roberts, S. M., Ed. *Preparative Biotransformations*, Wiley: New York, 1992–1998.

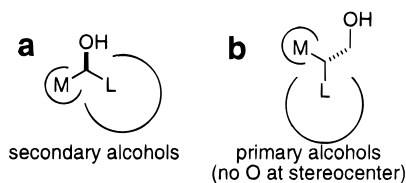


**Figure 1.** Empirical rules summarize the enantioselectivity of PCL toward chiral alcohols. (a) Shape of the favored enantiomer of secondary alcohols. M represents a medium-sized substituent, e.g.,  $\text{CH}_3$ , and L represents a large substituent, e.g., Ph. (b) Shape of the favored enantiomer of primary alcohols. This rule for primary alcohols is reliable only when the stereocenter lacks an oxygen atom. Note that the OH of secondary alcohols points toward the reader, while the  $\text{CH}_2\text{OH}$  of primary alcohols points away from the reader.

with hydrophobic side chains and open to the solvent. The other pocket is medium-sized and contains polar as well as hydrophobic side chains.

Researchers used computer modeling of transition state analogues bound to lipases to confirm the molecular recognition model suggested in Figure 1.<sup>7,5b</sup> This modeling starts with the X-ray structure of the lipase, docks into it a tetrahedral intermediate or transition state analogue, and minimizes the energy of the complex. A productive complex is one that has all the hydrogen bonds required for catalysis and a good fit within the active site. Such modeling usually correctly predicts the fast-reacting enantiomer, but quantitative prediction of enantioselectivity remains difficult. The slow enantiomer either does not fit as well into the active site or fits in a nonproductive manner.

Understanding the molecular recognition of primary alcohols has been more difficult. First, most lipases show low enantioselectivity toward primary alcohols. Only lipase from *Pseudomonas cepacia* (PCL) and lipase from porcine pancreas (PPL) show moderate to high enantioselectivity toward a wide range of primary alcohols, but even for these the enantioselectivity is usually lower than toward secondary alcohols. Second, a simple rule based on the size of the substituents cannot predict the favored enantiomer for all primary alcohols. For PPL, researchers working with different substrates proposed opposite, enantiomeric rules! Of course, neither rule predicted the favored enantiomer for all substrates. For PCL, we found that a simple rule works if we exclude primary alcohols with an oxygen at the stereocenter, Figure 1.<sup>8</sup>

(5) (a) *Rhizomucor miehei* lipase: Ranghino, G.; Battistel, E.; Giovenco, S. *Trends QSAR Mol. Modell.* 92, *Proc. Eur. Symp. Struct.-Act. Relat.: QSAR Mol. Modell.*, 9th, 1992 (1993) (Wermuth, C.-G., Ed.; ESCOM: Leiden, NL) 1992, 373–378. (b) *Candida rugosa* lipase: Faber, K.; Griengl, H.; Hoenig, H.; Zuegg, J. *Biocatalysis* 1994, 9, 227–239. (c) Similar approach for *Pseudomonas cepacia* lipase: Lemke, K.; Lemke, M.; Theil, F. *J. Org. Chem.* 1997, 62, 6268–6273.

(6) Reviews: Dodson, G. G.; Lawson, D. M.; Winkler, F. K. *Faraday Discuss.* 1992, 95–105. Derewenda, Z. S. *Adv. Prot. Chem.* 1994, 45, 1–52. Cygler, M.; Grochulski, P.; Schrag, J. D. *Can. J. Microbiol.* 1995, 41, 289–96. Kazlauskas, R. J. *Trends Biotechnol.* 1994, 12, 464–72 (errata 1994, 13, 195).

(7) Secondary alcohols, HLL, RML, CRL: Norin, M.; Haeffner, F.; Achour, A.; Norin, T.; Hult, K. *Prot. Sci.* 1994, 3, 1493–1503. Sainz-Diaz, C. I.; Wohlfahrt, G.; Nogoceke, E.; Hernández-Laguna, A.; Smeyers, Y. G.; Menge, U. *Theochem, J. Mol. Struct.* 1997, 390, 225–237. Parve, O.; Vallikivi, I.; Metsala, A.; Lille, U.; Tougu, V.; Sikk, P.; Kaambre, T.; Vija, H.; Pehk, T. *Tetrahedron* 1997, 53, 4889–4900. Ema, T.; Kobayashi, J.; Maeno, S.; Sakai, T.; Utaka, M. *Bull. Chem. Soc. Jpn.* 1998, 71, 443–453. Faber, K.; Griengl, H.; Hoenig, H.; Zuegg, J. *Biocatalysis* 1994, 9, 227–239. CAL-B: Uppenberg, J.; Öhrner, N.; Norin, M.; Hult, K.; Patkar, S.; Waagen V.; Anthonsen, T.; Jones, T. A. *Biochemistry* 1995, 34, 16838–16851. Haeffner, F.; Norin, T.; Hult, K. *Biophys. J.* 1998, 74, 1251–1262.

In this paper, we use computer modeling to investigate the molecular basis of enantiomer recognition by PCL. We will address three questions. First, the models for primary alcohols and secondary alcohols suggest a reversal of enantioselectivity for PCL. In the fast-reacting enantiomer of secondary alcohols, the hydroxyl group faces toward the reader, but for the fast-reacting enantiomer of primary alcohols, the  $\text{CH}_2\text{OH}$  group points into the plane of the paper. Computer modeling will show that the large substituents of primary and secondary alcohols bind in different regions of PCL. This difference in binding accounts for the reversal of enantioselectivity.

The second question is why primary alcohols with an oxygen at the stereocenter do not follow the empirical rule. Of the 27 substrates collected in an earlier paper, only 10 fit the empirical rule; 31% agreement.<sup>8</sup> This is worse than guessing which gives 50% and suggests that this class of primary alcohols may follow an opposite empirical rule. The computer modeling will identify a hydrogen bond that can reverse the enantioselectivity for some primary alcohols with an oxygen at the stereocenter.

The last and most challenging question is how to increase the enantioselectivity of PCL toward primary alcohols. For secondary alcohols, increasing the difference in size of the substituents usually increases the enantioselectivity of lipase. However, previous work showed that this approach was not reliable for PCL-catalyzed reactions of primary alcohols. Sometimes it had no effect, sometimes it increased, and sometimes it decreased the enantioselectivity. The modeling below suggests a way to increase the enantioselectivity toward some alcohols by chemical modification to increase the strength of a key hydrogen bond.

Although the goal of this paper is to understand the molecular recognition of enantiomers of **1** and **2** by PCL, pure enantiomers of **1** and **2** are also useful for synthesis. For example, Delnick and Margolin noted that pure enantiomers of **1** would be useful for the synthesis of adenosine receptor agonists and antagonists,<sup>9</sup> while Heathcock and co-workers used (*R*)-**1** in the synthesis of the side chain of zaragozic acid A (squalestatin S1).<sup>10</sup> Wimmer et al. used pure enantiomers of **2** to prepare analogues of insect juvenile hormones,<sup>11</sup> and Dirlam et al. used a *p*-fluoro derivative to make sorbinil, an aldose reductase inhibitor.<sup>12</sup>

All computer modeling in this paper begins with the X-ray crystal structure of the open conformation of PCL, which was recently reported by four groups.<sup>13</sup> Like other lipases, PCL is an  $\alpha/\beta$  hydrolase.<sup>14</sup> Ser87, His286, and Asp264 form the catalytic triad, while the amide hydrogens of Leu17 and Gln88 also contribute to catalysis by hydrogen bonding to the oxyanion intermediate.

(8) Weissfloch, A. N. E.; Kazlauskas, R. J. *J. Org. Chem.* 1995, 60, 6959–6969.

(9) Delnick, D. L.; Margolin, A. L. *Tetrahedron Lett.* 1990, 31, 6797–6798.

(10) Stoermer, D.; Caron, S.; Heathcock, C. H. *J. Org. Chem.* 1996, 61, 9115–9125.

(11) Wimmer, Z.; Saman, D.; Francke, W. *Helv. Chim. Acta* 1994, 77, 502–508.

(12) Dirlam, N. L.; Moore, B. S.; Urban, F. J. *J. Org. Chem.* 1987, 52, 3587–3591.

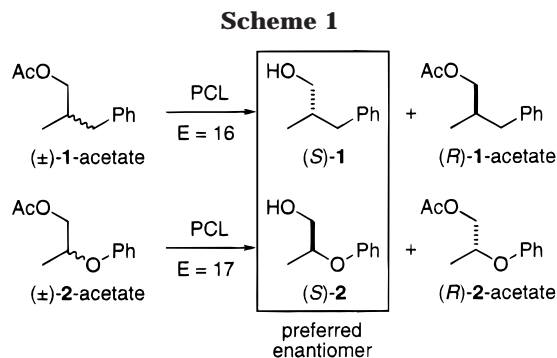


**Table 1. Enantioselectivity of PCL and Acetylated PCL toward Acetates of 1 and 2**

substrate	enzyme	ee <sub>p</sub> , %	ee <sub>s</sub> , %	E <sup>a</sup>
1-acetate	PCL	79	nd	16 (S) <sup>b</sup>
2-acetate	PCL	73	86	17 (S) <sup>c</sup>
2-acetate	PCL-nitrated <sup>d</sup>	40	92	36 (S)
2-acetate	PCL-acetylated <sup>e</sup>	50	89	8 (S)
2-acetate	PCL-deacetylated <sup>f</sup>	94	24	42 (S)

<sup>a</sup> The enantiomeric ratio measures the relative rate of hydrolysis of the fast enantiomer as compared to the slow enantiomer as defined by Sih (Chen, C. S.; Fujimoto, Y.; Girdaukas, G.; Sih, C. J. *J. Am. Chem. Soc.* **1982**, *104*, 7294–7299). The absolute configuration of the favored enantiomer is indicated in parentheses. <sup>b</sup> Data from ref 8. <sup>c</sup> The absolute configuration was determined by chemical correlation. The product alcohol was oxidized using Jones reagent, and the HPLC chromatogram (Chiracel OD column) of the resulting acid was compared to that previously reported (ref 35). <sup>d</sup> PCL was chemically modified by nitration with tetrani-tromethane. <sup>e</sup> PCL was chemically modified by acetylation with *N*-acetylimidazole. We estimate that 10 of the 14 tyrosine residues were acetylated. <sup>f</sup> The sample of acetylated PCL was treated with hydroxylamine to remove all *O*-acetyl groups.

## Results

**Enantioselectivity and Reversed Enantiopreference.** Lipase from *Pseudomonas cepacia* (PCL)<sup>15</sup> catalyzes the enantioselective hydrolysis of the acetate esters of **1** and **2**, Scheme 1, Table 1. The enantioselectivity (relative rate of hydrolysis of the fast enantiomer as compared to the slow enantiomer) is moderate for both acetates: 16 for **1**-acetate and 17 for **2**-acetate. In both cases, PCL favors the (*S*)-enantiomer, but, due to changes in the priorities of the substituents, the (*S*)-enantiomers of **1** and **2** have the opposite shapes. The fast-reacting enantiomer of **1** has the shape predicted by the rule in Figure 1b. The shape of the fast-reacting enantiomer of **2** does not fit the rule in Figure 1b. This lack of agreement for **2** is not surprising since we previously reported that the rule is not reliable for primary alcohols such as **2** that contain an oxygen at the stereocenter.

### Conformational Analysis of Unbound Substrates.

To find the reason for the opposite enantiopreference of PCL toward **1**- and **2**-acetate, we first compared the ground state conformations of the two substrates (details

(13) Kim, K. K.; Song, H. K.; Shin, D. H.; Hwang, K. Y.; Suh, S. W. *Structure* **1997**, *5*, 173–185. Schrag, J. D.; Li, Y. G.; Cygler, M.; Lang, D. M.; Burgdorf, T.; Hecht, H. J.; Schmid, R.; Schomburg, D.; Rydel, T. J.; Oliver, J. D.; Strickland, L. C.; Dunaway, C. M.; Larson, S. B.; Day, J.; McPherson, A. *Structure* **1997**, *5*, 187–202.

(14) Ollis, D. L.; Cheah, E.; Cygler, M.; Dijkstra, B.; Frolow, F.; Franken, S. M.; Harel, M.; Remington, S. J.; Silman, I.; Schrag, J. Sussman, J. L.; Verschueren, K. H. G.; Goldman, A. *Prot. Engineer.* **1992**, *5*, 197–211.

(15) Microbiologists recently renamed the bacterial species *Pseudomonas cepacia* as *Burkholderia cepacia*, but we continue to use the older name in this paper.

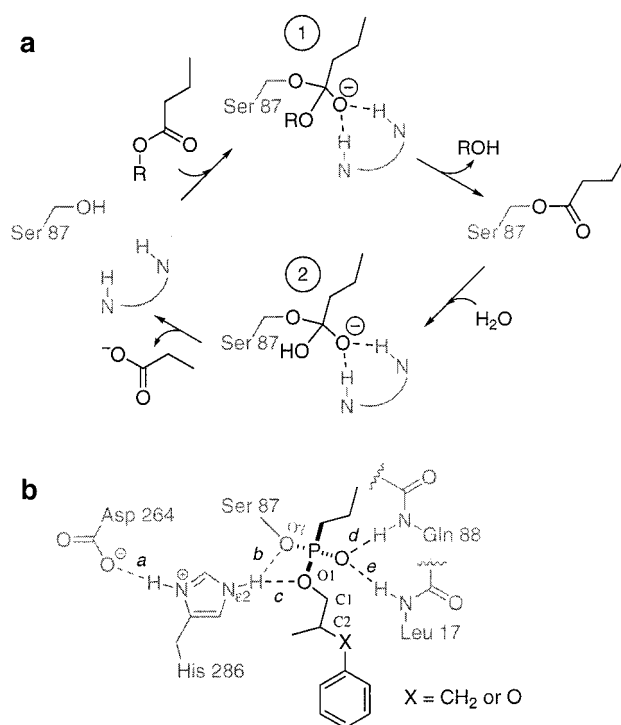


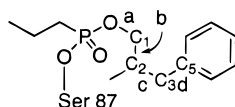
**Figure 2.** Intermediates and their analogues in the lipase-catalyzed hydrolysis of esters. Amino acids correspond to those in PCL. (a) In the accepted mechanism for hydrolysis of esters, the catalytic serine (Ser 87) attacks the ester once it binds in the active site. This attack forms the tetrahedral intermediate marked ①. Hydrogen bonds from two amide N–H's stabilize the oxyanion in this intermediate. Collapse of tetrahedral intermediate ① releases the alcohol and forms an acyl enzyme intermediate. The formation and collapse of tetrahedral intermediate ① determine the selectivity of a lipase toward the alcohol moiety of an ester. Attack of water on the acyl enzyme yields tetrahedral intermediate ②. Collapse releases the acid and regenerates the free enzyme. (b) A phosphonate mimics the transition states for formation and collapse of tetrahedral intermediate ①. Five hydrogen bonds, marked a–e, stabilize the charges. To be judged catalytically competent, the minimized structures must contain all five hydrogen bonds.

in Supporting Information). These calculations show that both **1**- and **2**-acetate are flexible without a well-defined conformation in solution. Both substrates easily adopt similar conformations. Thus, conformational preferences of the substrates do not cause the reversal in enantioselectivity of PCL. Different interactions of **1**- and **2**-acetate with the active site of PCL likely cause this reversal.

**Molecular Modeling of Transition State Analogues Bound to PCL.** The first chemical step in lipase-catalyzed ester hydrolysis is the attack of the active site serine at the ester carbonyl forming a tetrahedral intermediate, Figure 2a. Collapse of this tetrahedral intermediate releases the alcohol. The transition state involved in formation or collapse of this first tetrahedral intermediate defines the selectivity of PCL toward alcohols. To mimic this transition state for hydrolysis of butyrate esters of **1** or **2**, we used the phosphonates linked to PCL shown in Figure 2b. Indeed, researchers have shown that phosphonates mimic well the transition state for ester hydrolysis.<sup>16</sup>

To search for stable conformations, we systematically minimized all nine possible conformations along bonds b and c (see structures in Tables 2 and 3).<sup>17</sup> We did not vary the dihedral angle along bond a because the active

Table 2. Stable Conformations of Transition State Analogs for the PCL-Catalyzed Hydrolysis of 1-Butyrate



structure name	dihedral angles, <sup>a</sup> deg (bonds b, c)	E <sup>b</sup> (kcal/mol)	no. of H-bonds <sup>c</sup>	acid <sup>d</sup>	productive
(S)-1-PCL-a	-175, 176	0, 8	5	Glu289	yes
(S)-1-PCL-b	85, 78	6	6 <sup>e</sup>	Asp264, Glu289	yes
(S)-1-PCL-c	-60, 176	2, 3, 6	4 <sup>f</sup>	Glu289	maybe <sup>g</sup>
(S)-1-PCL-d	75, -110	17	3 <sup>h</sup>	Asp264	no
(S)-1-PCL-e	-164, -59	21	4 <sup>f</sup>	Asp264	no
(S)-1-PCL-f	-85, 53	9	1 <sup>i</sup>	-	no
(R)-1-PCL-a	-177, -169	13	5	Asp264	yes
(R)-1-PCL-b	58, -160	20	5	Glu289	yes
(R)-1-PCL-c	158, 76	28	5	Glu289	yes
(R)-1-PCL-d	-63, -158	0, 7	4 <sup>f</sup>	Glu289	no
(R)-1-PCL-e	-67, 93	5	3 <sup>h</sup>	Glu289	no
(R)-1-PCL-f	52, -76	7	3 <sup>h</sup>	Asp264	no
(R)-1-PCL-g	58, 56	17	3 <sup>h</sup>	Glu289	no
(R)-1-PCL-h	175, -48	19	3 <sup>h</sup>	Asp264	no

<sup>a</sup> Dihedral angle for bond b is defined by O-C<sub>1</sub>-C<sub>2</sub>-C<sub>3</sub>. The dihedral angle for bond c is defined by C<sub>1</sub>-C<sub>2</sub>-C<sub>3</sub>-C<sub>5</sub>. <sup>b</sup> Different initial conformations sometimes converged to the same final structure, but with different energy values. Each energy value is listed. <sup>c</sup> The transition state in Figure 2b requires five hydrogen bonds. <sup>d</sup> PCL contains redundant acid moieties for the catalytic triad: Asp264 and Glu289. <sup>e</sup> His 286 forms a bifurcated hydrogen bond to both Asp264 and Glu289. <sup>f</sup> The hydrogen bond between His286 and the substrate oxygen was missing. <sup>g</sup> The missing hydrogen bond may be a weak hydrogen bond. <sup>h</sup> Hydrogen bonds between His286 and Ser87 and between His286 and the substrate oxygen are missing. <sup>i</sup> All hydrogen bonds are missing except for one between phosphoryl oxygen and Leu17.

site fixed this angle near 180°. A productive conformation requires the phosphoryl oxygen (oxyanion mimic) in the oxyanion hole and the alcohol oxygen within hydrogen bonding distance of His286. These requirements fix the dihedral angle along bond a near 180°. The dihedral angle along bond d varied significantly during minimization, so we did not vary it manually. In addition, we manually constructed several reasonable structures and minimized them. Ideally, all starting conformations should converge to one, lowest energy minimum. In practice, some conformations converge, but others do not. The results of the calculations are several local minima, each of which must be judged for catalytic competence. Tables 2 and 3 summarize the stable conformations.

One conclusion was obvious. The large substituent of primary alcohols did not bind as expected in the large hydrophobic pocket. Previous work on secondary alcohols identified a large and a medium hydrophobic pocket in the alcohol-binding site of lipases.<sup>18,7</sup> The large pocket lies above the active site serine in the view shown in Figures 3 and 4, while the medium pocket lies below the active site serine. As expected the medium substituents of **1** and **2**, CH<sub>3</sub>, lies in, or near, the medium-sized binding pocket analogous to that postulated for secondary alco-

hols. However, the large substituent of the primary alcohols (CH<sub>2</sub>Ph or OPh) did not bind in the large hydrophobic pocket. In all calculated minima, this large pocket is empty or nearly empty. Instead, the CH<sub>2</sub>Ph or OPh groups usually bind in a narrow groove at the base of the active site. We call this groove the alternate hydrophobic pocket. It is also lined with hydrophobic amino acids—Tyr23, Leu27, Tyr29, Phe146, Ile290, and Leu293. (In a few nonproductive structures, the CH<sub>2</sub>Ph or OPh groups lie outside this pocket, but no structure showed the CH<sub>2</sub>Ph or OPh groups within the large hydrophobic pocket.) Thus, the large substituents of primary and secondary alcohols bind to different pockets in PCL. Other researchers have also suggested that PCL contains two hydrophobic pockets on the basis of substrate mapping.<sup>19</sup>

**Method for Identifying Best Productive Conformations.** We used two criteria to identify which local minima were catalytically relevant. First, we looked for the five hydrogen bonds required for catalysis, see Figure 2b. To assign a hydrogen bond, we looked, first, for a donor to acceptor atom distance of less than 3.1 Å. Second, we looked for a nearly linear arrangement of donor atom, hydrogen, and acceptor atom. We considered an angle of 120° or more as nearly linear. These are relatively generous limits for a hydrogen bond. We classified any structure lacking two or more of the five hydrogen bonds as nonproductive. However, if a structure lacked only one hydrogen bond and it was only slightly outside the limits set above, then we classified it as maybe productive.

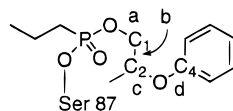
PCL contains redundant acids for the catalytic triad, Asp264 and Glu289. The catalytic histidine, His286, lies near both acids and can hydrogen bond to either one or both acids. The closely related lipase from *Pseudomonas glumae* also contains redundant acids: Asp263 and

(16) Phosphonates strongly inhibit hydrolases; for example, Hanson, J. E.; Kaplan, A. P.; Bartlett, P. A. *Biochemistry* **1989**, *28*, 6294–6305. Antibodies to phosphonates often catalyze hydrolysis of the corresponding esters; for example, Jacobs, J.; Schultz, P. G.; Sugawara, R.; Powell, M. *J. Am. Chem. Soc.* **1987**, *109*, 2174–2176.

(17) Although some researchers used molecular dynamics to search conformations of ligand–protein complexes, we found that molecular dynamics searched too small a region of conformational space. For example, starting from a structure of (S)-1-PCL with bond angles of -74° and 75° (bonds b and c, respectively), a long molecular dynamics run (300 K for 1 ps for the equilibration period and 25 ps for the simulation) shifted torsion angles by less than 20°. However, upon energy minimization, this conformation relaxed to torsion angles of -60° and 176° (structure (S)-1-PCL-c in Table 1). For this reason, we used a systematic search to more completely search for productive conformations.

(18) Cygler, M.; Grochulski, P.; Kazlauskas, R. J.; Schrag, J. D.; Bouthillier, F.; Rubin, B.; Serreqi, A. N.; Gupta, A. K. *J. Am. Chem. Soc.* **1994**, *116*, 3180–3186.

(19) (a) Hof, R. P.; Kellogg, R. M. *J. Chem. Soc., Perkin Trans. 1* **1996**, 2051–2060. (b) Lemke, K., Lemke, M., Theil, F. *J. Org. Chem.* **1997**, *62*, 6268–6273.

**Table 3. Stable Conformations of Transition State Analogs for the PCL-Catalyzed Hydrolysis of 2-Butyrate**

structure name	dihedral angles, <sup>a</sup> deg (bonds b, c)	<i>E</i> <sup>b</sup> (kcal/mol)	no. of H-bonds <sup>c</sup>	acid <sup>d</sup>	productive
( <i>S</i> )-2-PCL-a	-161, -153	5	4 <sup>e,f</sup>	Asp264	maybe
( <i>S</i> )-2-PCL-b	-44, -65	18	4 <sup>f,g</sup>	Asp264	maybe
( <i>S</i> )-2-PCL-c	48, -168	8, 13	4 <sup>f,h</sup>	Asp264	maybe
( <i>S</i> )-2-PCL-d	-77, -166	0	3 <sup>i</sup>	Glu289	no
( <i>S</i> )-2-PCL-e	-179, -78	22	3 <sup>i</sup>	Asp264	no
( <i>S</i> )-2-PCL-f	159, 71	16	2 <sup>j</sup>	—	no
( <i>S</i> )-2-PCL-g	61, 79	2	1 <sup>k</sup>	—	no
( <i>R</i> )-2-PCL-a	-155, 176	7, 11	6 <sup>l</sup>	Asp264	yes
( <i>R</i> )-2-PCL-b	83, 86	19	5	Asp264	yes
( <i>R</i> )-2-PCL-c	-61, 145	2, 3, 9	4 <sup>e,f</sup>	Asp264	maybe
( <i>R</i> )-2-PCL-d	-159, -64	13	4 <sup>e,f</sup>	Asp264	maybe
( <i>R</i> )-2-PCL-e	79, 59	19	4 <sup>e</sup>	Glu289	no
( <i>R</i> )-2-PCL-f	-53, -76	0	2 <sup>m</sup>	Asp264	no

<sup>a</sup> Dihedral angle for bond b is defined by O-C<sub>1</sub>-C<sub>2</sub>-O. The dihedral angle for bond c is defined by C<sub>1</sub>-C<sub>2</sub>-O-C<sub>4</sub>. <sup>b</sup> Different initial conformations sometimes converged to the same final structure, but with different energy values. Each energy value is listed. <sup>c</sup> The transition state in Figure 2b requires five hydrogen bonds. <sup>d</sup> PCL contains redundant acid moieties for the catalytic triad: Asp264 and Glu289. <sup>e</sup> The hydrogen bond between His286 and Ser87 is missing. <sup>f</sup> The missing hydrogen bond may be a weak hydrogen bond. <sup>g</sup> The hydrogen bond between His286 and the substrate oxygen was missing. <sup>h</sup> Two minimizations of this conformation gave slightly different hydrogen bonding patterns. In one minimization, the hydrogen bond between His286 and the alcohol oxygen was weak, but the hydrogen bond between His286 and Asp264 was present. In the other minimization, both of these bonds were weak. <sup>i</sup> Hydrogen bonds between His286 and Ser87 and between His286 and the substrate oxygen are missing. <sup>j</sup> All hydrogen bonds are missing except for the two bonds between the phosphoryl oxygen and Leu17 and the phosphoryl oxygen Gln88. <sup>k</sup> All hydrogen bonds are missing except for one between phosphoryl oxygen and Leu17. <sup>l</sup> In addition to the five catalytically essential hydrogen bonds, this structure also shows an additional hydrogen bond between the phenoxy oxygen of the substrate and the phenolic hydroxyl of Tyr29. <sup>m</sup> Only hydrogen bonds between His286 and Asp264 and between the phosphoryl oxygen and Leu17.

Glu288.<sup>20</sup> Mutation of Asp263 to Ala yielded a lipase with 25% of the original activity, showing that Glu288 can serve as the acid in the catalytic triad. For this reason, we accepted a hydrogen bond from His286 to either of Asp264 or Glu289 as productive.

The second requirement for catalytically relevant minima was good binding of the alcohol moiety in the active site. We made this judgment qualitatively and picked minima that bound the methyl and phenyl groups of the alcohol more completely. In addition, we avoided binding modes that required extensive rearrangement of the side chains within the active site.

We did not use calculated energies to judge whether a conformation was catalytically relevant because we found the calculated energies unreliable. With large structures such as an enzyme, the sum of small differences, even those far from the active site, yields large differences in calculated energy. For example, in the minimization of (*S*)-1-PCL, three initial structures converged to the "same" final structure, labeled (*S*)-1-PCL-c in Table 2. The geometry of the transition state analogue was identical in all three, but the calculated energies differed by 4 kcal/mol. Unnoticed differences in the protein residues or solvent molecules caused this difference in energy. Similarly, for (*S*)-1-PCL-a in Table 2 the calculated energy of two apparently identical structures differed by 8 kcal/mol.

#### Catalytically Relevant Conformations of 1-PCL

Among the six calculated minima for (*S*)-1-PCL, we identified two productive conformations, one possibly productive conformation, and three nonproductive conformations, Table 2. Of the two productive conformations,

(*S*)-1-PCL-a and -b, we favor conformation a as the catalytically competent one, Figure 3, because it has qualitatively better hydrophobic interactions. The methyl substituent lies in a shallow pocket between His86 and His286, while the phenyl ring lies in alternate hydrophobic pocket mentioned above. Conformation b is similar to a with the following differences. His286 turns between Asp264 and Glu289 and hydrogen bonds to both acid residues. The methyl points out of the active site toward the solvent and the phenyl ring is oriented deeper into the alternate hydrophobic pocket. To accommodate the phenyl ring, residues Ile290, Leu287, and Trp30 move from their original positions in the X-ray crystal structure. In conformation c, the methyl lies in the same pocket as in conformation a, while phenyl ring points out of the pocket, exposing one face to solvent. In addition, conformation c contains a weak hydrogen bond between His286 and the substrate oxygen. The nitrogen-oxygen distance of 3.05 Å is within the accepted range, but the N-H-O angle of 104° is too acute.

Conformations d and f lack four and two of the five catalytically important hydrogen bonds, respectively, and are thus nonproductive. Conformation e lacks only one hydrogen bond, but the nitrogen-oxygen distance of 3.42 Å is larger than expected for even a weak hydrogen bond. Thus, conformation e is also nonproductive. The N-H-O angle of 135° is within the accepted range.

For (*R*)-1, we found three productive conformations and five nonproductive conformations. As with (*S*)-1, all conformations bind the benzyl group, not in the large hydrophobic pocket, but in the alternate hydrophobic pocket. The three productive conformations, a-c, all contain the five catalytically essential bonds, but none of the three makes good hydrophobic contacts between the lipase and both the methyl and benzyl substituents.

(20) Noble, M. E. M.; Cleasby, A.; Johnson, L. N.; Egmond, M. R.; Frenken, L. G. J. *FEBS Lett.* **1993**, *331*, 123-128.

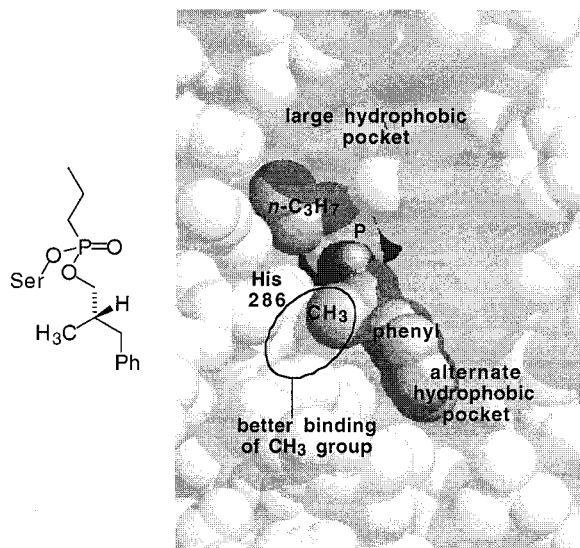


**Figure 3.** Catalytically competent orientation of the phosphonate transition state analogue for the PCL-catalyzed hydrolysis of (*S*)-**1** butanoate as identified by molecular modeling. Atoms from the lipase are shown in light gray, while atoms from the phosphonate are in light gray (phosphorus), dark gray (carbons), and darkest gray (oxygen). For clarity, all hydrogen atoms and water molecules are hidden. On the basis of previous work with secondary alcohols, we expected the large substituent of this primary alcohol ( $\text{CH}_2\text{Ph}$ ) to bind in the large hydrophobic pocket. However, modeling found an alternate binding pocket. This binding mode maintains all the catalytically essential hydrogen bonds identified in Figure 2b. In the fast-reacting enantiomer, shown above, the methyl group nestles into a hydrophobic pocket created in part by the catalytic histidine (His 286). The slow reacting enantiomer (not shown) shows an identical orientation, except the hydrogen and methyl groups at the stereocenter have exchanged positions. This exchange removes the methyl group from the hydrophobic pocket and leaves it solvent-exposed. Thus, modeling predicts that the fast-reacting enantiomer binds better to PCL.

Of the three conformations, conformation a makes the best hydrophobic contacts. It binds the phenyl ring well within the alternate binding pocket, but the methyl group lies without hydrophobic contacts and points toward the opening of the active site pocket. In conformation c, the methyl group lies without hydrophobic contacts as in conformation a. The benzyl group twists within the alternate hydrophobic pocket, thereby losing hydrophobic contacts to Tyr23 and Tyr29. In conformation b, the methyl lies in the alternate hydrophobic pocket and the benzyl substituent points toward the medium sized pocket, but is too large to bind in it. The phenyl ring loses all hydrophobic contacts. Since conformation a makes the best hydrophobic contacts, it will be considered the catalytically relevant conformations.

Conformation d is nonproductive because it lacks the hydrogen bond between His286 and the substrate oxygen. The distances are too long with N–O distance of 3.58 Å and the N–H–O angle of 89° is too acute. Conformations e–h lack two hydrogen bonds and are therefore nonproductive.

Thus, the major difference between transition states for esters of (*S*)-**1** and (*R*)-**1** is the binding of the methyl group (the medium substituent). For esters of preferred enantiomer, (*S*)-**1**, the methyl group binds in a hydrophobic pocket, but for esters of (*R*)-**1** it lies outside this pocket.

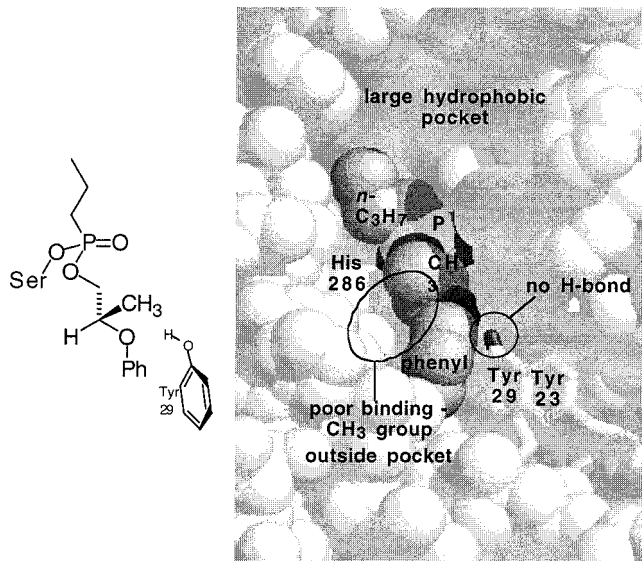


**Figure 4.** Catalytically competent orientation of the phosphonate transition state analogue for the PCL-catalyzed hydrolysis of (*S*)-**2** butanoate as identified by molecular modeling. Atoms from the lipase are shown in light gray, while atoms from the phosphonate are in light gray (phosphorus), dark gray (carbons), and darkest gray (oxygen). For clarity, all hydrogen atoms and water molecules are hidden, and two amino acid residues, Tyr 23 and Tyr 29, are shown in the stick representation. In addition, the phenolic oxygen atom of Tyr 29 is colored darkest gray. This binding mode maintains all the catalytically essential hydrogen bonds identified in Figure 2b. The binding mode of the fast-reacting enantiomer, shown above, is similar to that shown for (*S*)-**1** butanoate in Figure 3. The large substituent (OPh) binds in the alternate hydrophobic pocket. The oxygen of the OPh group lies near the phenolic oxygen of Tyr 29 (O–O distance 2.84 Å), but does not form a hydrogen bond since the O–H–O bond angle (98°) is too acute. The slow-reacting enantiomer (not shown) shows two differences. First, the hydrogen and methyl at the stereocenter have exchanged positions. This exchange nestles the methyl group into the hydrophobic pocket. Thus, modeling predicts that the slow enantiomer bind better. Second, a hydrogen bond forms between the oxygen of OPh and the phenolic oxygen of Tyr 29 (O–O distance 3.04 Å, O–H–O angle = 131°) due to subtle rearrangements of the structure. The hydrogen bond probably slows down the release of the alcohol.

#### Catalytically Relevant Conformation of 2–PCL.

For (*S*)-**2**, we found three possibly productive and four nonproductive conformations, Table 3. The possibly productive conformations, a–c, contained one weak hydrogen bond. For conformation a, the hydrogen bond between His286 and Ser87 is weak: the N–O distance is 3.32 Å and the N–H–O bond angle is 123°. For conformation b, the hydrogen bond between His286 and alcohol oxygen was weak: the N–O distance is 3.01 Å and the N–H–O bond angle is 140°. Conformation c gave slightly different hydrogen bonding patterns in two different minimizations. In one minimization, the hydrogen bond between His286 and the alcohol oxygen was weak (the N–O distance is 3.33 Å and the N–H–O bond angle is 141°). In the other minimization, hydrogen bonds between His286 and the alcohol oxygen and between His286 and Asp264 were both weak.

Of the three possibly productive conformations, (*S*)-**2**–PCL-a shows the best hydrophobic interactions with the substrate. This conformation resembles (*R*)-**1**–PCL-a above. The benzyl group binds in the alternate hydro-

phobic pocket while the methyl group lies without hydrophobic contacts and points toward the opening of the active site pocket. In conformation b the methyl group binds in the medium pocket, while the phenyl group points toward the large hydrophobic pocket. The phenyl group does not reach the hydrophobic pocket and has no hydrophobic interactions with PCL. In conformation c the methyl lies in the alternate hydrophobic pocket and the benzyl substituent points toward the medium sized pocket, but is too large to bind in it. The phenyl ring loses all hydrophobic contacts. None of these three conformations is clearly best. The hydrogen bond appears stronger for b and c, while the hydrophobic interactions are definitely stronger for a. We chose conformation a as the catalytically relevant conformation, but most of the interpretation below would remain the same if we had chosen conformations b or c.

Conformations d–g lack two to four hydrogen bonds and are therefore nonproductive.

For (*R*)-**2**, we found two productive conformations, two possibly productive conformations and two nonproductive conformations. The two productive conformations, a and b, have all five catalytically essential hydrogen bonds. The two possibly productive conformations, c and d, have a weaker hydrogen bond between His286 and Ser87 (c: N–O distance is 3.27 Å, N–H–O angle is 131°; d: 3.18 Å and 124°, respectively).

Of these four conformations, (*R*)-**2**–PCL-a shows the best hydrophobic interactions. It binds the methyl group of (*R*)-**2** in the medium-sized pocket and the benzyl group in the alternate hydrophobic pocket. Conformation b leaves the methyl group outside the hydrophobic pocket. Accommodating the benzyl group also required rearrangement of the amino acid side chains. Conformation c has the medium-sized substituent oriented toward the alternate hydrophobic pocket and the large substituent partly in the medium-sized pocket. One face of the phenyl ring is open to the solvent. Conformation d has the methyl substituent bound in the medium-sized pocket. The large substituent is bound within the alternate hydrophobic pocket, but in a manner that causes significant rearrangement of the amino acid side chains. Thus, we believe conformation a is the catalytically relevant conformation because it contains all necessary hydrogen bonds and qualitatively shows the best hydrophobic interactions in the active site.

Further, conformation a of (*R*)-**2**–PCL shows an additional hydrogen bond between the phenolic hydroxyl of Tyr29 and the phenoxy oxygen of the substrate (O–O distance of 3.04 Å, O–H–O angle of 131°). None of the other conformations for either (*S*)-**2** or (*R*)-**2** formed this hydrogen bond. This bond may explain the slower hydrolysis of esters of (*R*)-**2**, see below. The catalytically relevant conformation for the fast-reacting enantiomer, (*S*)-**2**–PCL-a, lacks this hydrogen bond, but there may be a weak interaction. The distances are suitable (the O–O distance is 2.84 Å), but the angle is too acute (O–H–O angle is 98°).

Conformation (*R*)-**2**–PCL-e is nonproductive because it lacks the hydrogen bond between His286 and Ser87. The N–O distance is 3.42 Å, and the N–H–O angle is 136°. These distances are too far for a hydrogen bond. Conformation (*R*)-**2**–PCL-f is nonproductive because it lacks three hydrogen bonds.

Thus, the two major differences between transition states for esters of (*S*)-**2** and (*R*)-**2** are the orientation of

**Table 4. Kinetic Parameters for PCL-Catalyzed Hydrolysis of Enantiomers of 1-Acetate and 2-Acetate<sup>a</sup>**

substrate	$k_{\text{cat}}$ (min <sup>-1</sup> )	$K_m$ (mM)	$k_{\text{cat}}/K_m$ (M <sup>-1</sup> min <sup>-1</sup> )
( <i>S</i> )- <b>1</b> -acetate	4.7 ± 2.1	28 ± 1	170
( <i>R</i> )- <b>1</b> -acetate	3.2 ± 0.4	300 ± 140	11
( <i>S</i> )- <b>2</b> -acetate	480 ± 150	33 ± 12	15000
( <i>R</i> )- <b>2</b> -acetate	5.0 ± 0.8	6 ± 4	830

<sup>a</sup> Kinetic constants were determined by the method of Hwang et al. (ref 36). This method fits the observed degree of conversion as a function of time with the previously measured enantiomeric ratios (Table 1). Since the substrate was not completely dissolved in the reaction mixture, the values of  $K_m$  are apparent values.

the methyl group and the “extra” hydrogen bond. For esters of preferred enantiomer, (*S*)-**2**, the methyl group lies outside the hydrophobic pocket, and no hydrogen bond forms between the phenoxy oxygen and the phenol OH of Tyr29. In contrast, for esters of (*R*)-**2**, the methyl group binds in the hydrophobic pocket, and a hydrogen bond does form between the phenoxy oxygen and the phenol OH of Tyr29.

**Determination of Kinetic Constants.** To help interpret the results from molecular modeling, we measured the kinetic constants for **1**-acetate and **2**-acetate, Table 4. For **1**-acetate, the values of  $k_{\text{cat}}$  are similar for both enantiomers, but the values for  $K_m$  differ by approximately a factor of 10. In most cases, researchers treat  $K_m$  as a binding constant. Thus, PCL favors the (*S*)-enantiomer of **1**-acetate because it binds better than the (*R*)-enantiomer. Modeling suggests that in the catalytically relevant conformation, the methyl group in (*S*)-**1** binds in the medium pocket, while the methyl group of (*R*)-**1** does not. For these reasons, we propose that binding of the methyl group within the medium pocket determines the enantioselectivity of PCL for esters of (*S*)-**1**.

For **2**-acetate, both  $k_{\text{cat}}$  and  $K_m$  differ significantly for the enantiomers. The value of  $k_{\text{cat}}$  is approximately 100 times larger for the preferred (*S*)-**2**-acetate than for the (*R*)-**2**-acetate. On the other hand, the preferred (*S*)-enantiomer binds less tightly to PCL; the value of  $K_m$  is approximately five times higher for (*S*)-**2**-acetate than for (*R*)-**2**-acetate. Thus, binding differences favor the (*R*)-enantiomer while reaction rate differences favor the (*S*)-enantiomer. Since the differences in reaction rate are larger than differences in binding constant, PCL favors (*S*)-**2**-acetate. Nishizawa et al.<sup>21</sup> measured similar kinetic constants for a related substrate, 2-methyl-2-(4-phenoxyphenoxy)ethyl acetate, with PCL. The structure is the same as **2**-acetate, but with an added *p*-phenoxy group. The measured value of  $k_{\text{cat}}$  is eight times larger for the (*S*)-enantiomer (18 vs 2.2 min<sup>-1</sup> for (*R*)), but the value of  $K_m$  is also one and a half times larger for the (*S*)-enantiomer (6.8 vs 4.9 mM). Thus, as for **2**,  $k_{\text{cat}}$  favors the (*S*)-enantiomer, while  $K_m$  favors the (*R*) enantiomer. The overall enantioselectivity was 5.8 favoring the (*S*)-enantiomer.

The values of  $k_{\text{cat}}$  for the preferred enantiomer of **2** are much higher than for **1**. It is not readily apparent why **2** should react much faster than **1**.

Thus, kinetic measurements show that esters of (*S*)-**2** react faster, but bind more poorly. Modeling easily accounts for the poorer binding. The methyl group of (*S*)-**2** lies outside the hydrophobic pocket, but the methyl group of (*R*)-**2** lies inside this pocket. Modeling also suggests

(21) Nishizawa, K.; Ohgami, Y.; Matsuo, N.; Kisida, H.; Hirohara, H. *J. Chem. Soc., Perkin Trans. 2* **1997**, 1293–1298.

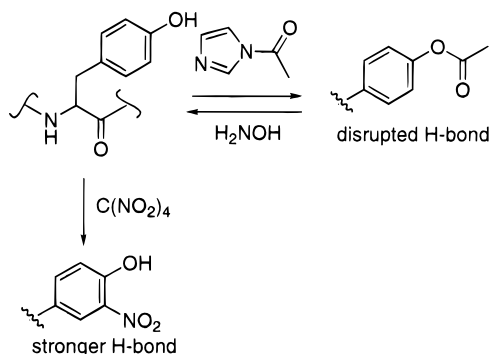


**Figure 5.** Chemical modification of tyrosyl residues. Acetylation of tyrosine residues disrupts any hydrogen bonds formed by the phenolic hydroxyl. Subsequent reaction with hydroxylamine removes the *O*-acetyl groups. Nitration of the tyrosyl residues increases the acidity of the phenolic hydroxyl and strengthens any hydrogen bonds involving this group. Chemical modification of enzymes is not selective for a particular position. All accessible tyrosines will be modified.

an explanation for the faster reaction of (*S*)-**2**. The “extra” hydrogen bond between phenolic OH of Tyr29 and the phenoxy oxygen of (*R*)-**2** may hold the leaving alcohol in place and promote the reverse reaction: breakdown to the starting ester. The overall effect would be to slow the forward reaction.

**Chemical Modification of Tyr29.** To test the importance of the phenolic OH of Tyr29 in the enantioselectivity of PCL toward **2**, we selectively modified the tyrosine hydroxyl groups by acetylation with *N*-acetyl-imidazole,<sup>22</sup> Figure 5. Acetylation will remove the “extra” hydrogen bond mentioned above. We predict that breaking this bond should lower the enantioselectivity of PCL toward **2**. However, acetylation also introduces a large group in the binding pocket. We cannot predict the effect of changing the size of the pocket. Another complication is that acetylation modified not only Tyr29, but an average of 10 of the 14 tyrosine residues in PCL. We cannot predict the effect of acetylating tyrosines other than Tyr29. With these cautions in mind, we observed a decrease in the enantioselectivity toward **2**-acetate from 17 (unmodified PCL) to 8 (acetylated PCL), Table 1 above.

We expected that the enantioselectivity of PCL toward **2**-acetate would return to 17 upon treatment with hydroxylamine to remove the *O*-acetyl groups from acetylated tyrosines.<sup>23</sup> However, the enantiomeric ratio increased more than expected to 42. This increase suggests an irreversible change occurred during chemical modification, perhaps acetylation of lysine residues or the *N*-terminal amino group.

We also modified PCL by nitration of the tyrosine residues with tetranitromethane to give 3-nitrotyrosyl residues, Figure 5. Nitration of tyrosine increases the acidity of the phenolic hydroxyl ( $pK_a$  drops from approximately 10.3 to 7.3). The increase acidity should increase the hydrogen bond-donating ability of Tyr29. Consistent with this expectation, the enantioselectivity toward **2**-acetate from 17 (unmodified PCL) to 37 (nitrated PCL), Table 1 above. Nitration modified on average 11 of the 14 tyrosine residues. The changes in

enantioselectivity upon acetylation and nitration are consistent with the proposed role of Tyr29, but, given the nonselective nature of chemical modification, they do not prove that the proposed role is correct.

## Discussion

Molecular modeling has identified an alternate binding pocket in PCL for the large substituent of alcohols **1** and **2**. The catalytically productive conformations of transition state analogues for hydrolysis of esters of (*S*)-**1**, (*R*)-**1**, (*S*)-**2**, and (*R*)-**2** all position the phenyl group within this alternate binding pocket. The X-ray structure of PCL clearly shows this pocket, and two previous substrate selectivity studies also suggest such a pocket.<sup>19</sup> The identification of an alternate binding pocket explains why PCL shows opposite enantiopreference toward primary and secondary alcohols. Primary and secondary alcohols bind differently. In secondary alcohols, the large substituent binds in the large pocket, but in primary alcohols, the large substituent binds in the alternate binding pocket.

Modeling and kinetics suggest that PCL recognizes the enantiomers of **1** by the binding of the methyl group. In the favored enantiomer, PCL binds the methyl group in a hydrophobic pocket, while in the unfavored enantiomer, the methyl group lies exposed to solvent. The maximum hydrophobic binding energy of a methyl group is 3.2 kcal/mol.<sup>23</sup> An enantiomeric ratio of 16 corresponds to an energy difference at 25 °C of 1.7 kcal/mol in the transition state for the two enantiomers. This value is consistent with partial hydrophobic binding for one enantiomer, but not the other. One way to increase the enantioselectivity of PCL toward **1** would be to make mutations that more completely bind the methyl group.

Modeling and kinetics also reveal why the enantioselectivity reverses for **2**. Although the binding of the methyl group favors (*R*)-**2**, this structure also contains an “extra” hydrogen bond between the phenoxy oxygen and Tyr29. The rate-determining step of serine esterase-catalyzed hydrolysis of esters is probably breakdown of the tetrahedral intermediate.<sup>24–26</sup> Slowing the release of alcohol would increase the chances for the reverse reaction—return to the starting ester. On the basis of the structure of a related lipase, lipase from *Chromobacterium viscosum*, without a bound transition state analogue, Lang et al. suggested that Tyr29 stabilizes the conformation of Glu288 (part of the catalytic triad) by hydrogen bonding through His86.<sup>27</sup> Loss of this stabilization when Tyr29 makes a hydrogen bond to the substrate may also explain the slower reaction of PCL with esters of (*R*)-**2**.

The identification of a hydrogen bond involved in enantiomer recognition of **2** also suggested a strategy to increase the enantioselectivity. Increasing the strength of this hydrogen bond should increase enantioselectivity, while decreasing the strength should decrease enantioselectivity. Indeed, chemical modification of PCL by nitration to increase the strength of the hydrogen bond

(22) Lundblad, R. L. *Techniques in Protein Modification*; CRC: Boca Raton, FL, 1995; pp 209–231.

(23) Fersht, A. *Enzyme Structure and Mechanism*, 2nd ed.; Freeman: New York, 1985; p 304.

(24) Nishizawa, K.; Ohgami, Y.; Matsuo, N.; Kisida, H.; Hirohara, H. *J. Chem. Soc., Perkin Trans. 2* **1997**, 1293–1298.

(25) Hirohara, H.; Philipp, M.; Bender, M. L. *Biochemistry* **1977**, *16*, 1573–1580.

(26) Hunkapiller, M. W.; Forgac, M. D.; Richards, J. H. *Biochemistry* **1976**, *15*, 5581–5588.

(27) Lang, D.; Hofmann, B.; Haalck, L.; Hecht, H. J.; Spener, F.; Schmid, R. D. *J. Mol. Biol.* **1996**, *259*, 704–717.



and acetylation to decrease the strength of the hydrogen bond changed the enantioselectivity in the expected direction. Although the magnitude of the change was modest (a factor of 2, approximately 0.4 kcal/mol), this is the first time that researchers have rationally increased the enantioselectivity of a lipase. Gu and Sih previously increased the enantioselectivity (typically from  $E = 2$  to 38) of lipase from *Candida rugosa* toward chiral acids upon nitration of the tyrosyl residues,<sup>28</sup> but they discovered this effect empirically. A number of other attempts to increase enantioselectivity by chemical modification were less successful. Modification of arginine in lipase from *Rhizomucor miehei* decreased or slightly increased (from  $E = 2.9$  to 4.4) the enantioselectivity toward esters of 2-methyldecanoic acid.<sup>29</sup> Acetylation of lysine residues in PCL either had no effect or decreased the enantioselectivity toward alcohols.<sup>30</sup>

These conclusions may hold for PCL-catalyzed reactions of other primary alcohols. For alcohols without an oxygen at the stereocenter, the alternate binding pocket would account for the reversed enantiopreference between primary and secondary alcohols. However, Zuegg et al. modeled several other primary alcohols in PCL,<sup>31</sup> but did not identify the "alternate binding pocket" discussed in this paper. Since primary alcohols are more flexible than secondary alcohols, there may be more than one explanation for the reversed enantiopreference.

When the primary alcohol contains an oxygen at the stereocenter, the situation is even more complex. Depending on the detailed structure, primary alcohols with an oxygen at the stereocenter may or may not make a hydrogen bond and thus may or may not follow the rule in Figure 1b. This "extra" hydrogen bond explains the difficulties researchers encountered in predicting the enantiopreference of PCL toward this class of alcohols.

The "extra" hydrogen bond identified in this paper may also contribute to the high selectivity of lipase from *Pseudomonas fluorescens* toward 1,2-diols of the type  $\text{HOCH}_2\text{C}(\text{OH})\text{RR}'$ , where reaction occurred at the primary alcohol.<sup>32,20a</sup> Researchers found that *Pseudomonas* lipase AK from Amano efficiently resolves a number of alcohols with that general structure. Although crystallographers have not yet solved the structure of this lipase, an alignment of its amino acid sequence with that of PCL suggest a tyrosine in the same position.<sup>33</sup> The OH at the stereocenter may also form a hydrogen bond to Tyr50 in lipase AK.

## Experimental Section

Lipase from *Pseudomonas cepacia* was purchased from Amano Enzyme Company (Lombard, IL) as LPL-200. This is a purified form of the lipase containing only protein and a small amount of glycine. For synthetic applications, less pure forms are suitable.

**2-Phenoxy-1-propanol Acetate, ( $\pm$ )-2 Acetate.** Acetic anhydride (0.60 mL, 6.75 mmol) was slowly added to a solution of ( $\pm$ ) 2-phenoxy-1-propanol (1.00 g, 6.57 mmol) and triethyl-

amine (0.94 mL, 6.75 mmol) in dichloromethane (5 mL). The reaction was stirred overnight under an atmosphere of nitrogen. The reaction mixture was washed with water ( $2 \times 5$  mL) and dried over  $\text{MgSO}_4$ . Evaporation of the solvent yielded pure product in 92% yield.

**Enantiomeric Ratio of PCL toward 2-Acetate.** A solution of PCL in phosphate buffer (2 mL, 10 mM, pH 7.5 or 8.0) was added to a mixture of distilled water (7 mL) and **2** (48 mg) dissolved in *tert*-butyl methyl ether (5 mL). The pH was maintained at either 7.5 or 8.0 with the addition of 0.0981 M NaOH controlled by a Radiometer RTS 822 pH stat. The reaction was stopped by adding 1.0 N HCl until the pH dropped to 1.8. The mixture was extracted with ethyl acetate ( $3 \times 10$  mL), and the combined organic extracts were dried with  $\text{MgSO}_4$ . The alcohol and acetate were separated by column chromatography on silica gel eluted with 1:4 ethyl acetate/hexane. The enantiomeric purity of the alcohol was measured by gas chromatography on a 30 m Chiraldex G-TA capillary column (Astec, Whippany, NJ): 2-phenoxypropanol: 90 °C 33.3 min (*R*), 34.0 min (*S*). The acetate was not well resolved on this column, so it was converted to the trifluoroacetate derivative for analysis: 2-phenoxypropanol trifluoroacetate: 80 °C, 22.1 min (*R*), 22.9 min (*S*). In some experiments a Chiralsil-Dex CB column (Chrompack, Middeburg, The Netherlands) was used (25 m, 110 °C) which separated enantiomers of both the alcohol and the acetate.

**Absolute Configuration of Favored Enantiomer of 2.** Jones reagent was added dropwise, until the yellow color persisted, to an acetone solution of 2-phenoxypropanol (36 mg) isolated from a PCL-catalyzed hydrolysis. After stirring for 1.5 h, the acetone was evaporated in vacuo and the residue was triturated with ethyl ether. The ether extract was washed with water. The aqueous layer was reextracted with ethyl ether, and the combined ethereal extracts were dried over magnesium sulfate. Purification of a portion by preparative TLC (8:2 cyclohexane/ethyl acetate,  $R_f = 0.12$ ) yielded 16 mg. HPLC analysis using a Chiracel OD column (90:10:1 hexane/2-propanol/formic acid) showed that the major enantiomer eluted first (major, 10.0 min; minor, 16.1 min) and thus was assigned the (*S*) configuration based on previous reports.<sup>34</sup>

**Kinetic Constants.** Values of  $K_m$  and  $k_{cat}$  were determined using the method of Hwang et al.<sup>35</sup> Briefly, we measured the degree of hydrolysis of the racemate as a function of time and, using the previously measured enantiomeric ratio, fit these data (nine to twelve points for each substrate) to the theoretical curve using Kaleidograph software. Lipase solution was added to a suspension of substrate (( $\pm$ )-1-acetate or ( $\pm$ )-2-acetate) in phosphate buffer (1 mL, 0.2 M, pH 7.0, 25 °C) stirred vigorously at 24 °C. At different reaction times, the reaction was stopped by lowering the pH to 2 with HCl (1 N). The reaction mixture was extracted with ethyl acetate ( $5 \times 0.8$  mL), and the combined organic extracts were dried over  $\text{MgSO}_4$ . The degree of hydrolysis was measured by GC (25 m Chirasil-Dex CB column, 140 °C, FID detector) and corrected for response factors of the alcohol and acetate. Enantiomers were not separated at this temperature. Since the substrate was not completely dissolved in the reaction mixture, the values of  $K_m$  are apparent values. Although true values of  $K_m$  could be calculated if we knew the partition coefficient of the substrate, both enantiomers have the same partition coefficient, so both the true and apparent  $K_m$ 's have the same relative values.

**Acetylation of PCL.** Solid *N*-acetylimidazole (300-fold molar excess) was added to a solution of PCL (100 mg in 20 mL in 0.010 M phosphate buffer, pH 7.5 with 5 vol % hexane to promote opening of the lipase lid). After stirring for 1 h, a 2.5 mL aliquot was desalted by passing through a gel filtration column (Pharmacia PD-10 column equilibrated with 0.01 M phosphate buffer, pH 7.5). Another 2.5 mL aliquot was deacetylated by adding hydroxylamine (1 M final concentra-

(28) Gu, Q.-M.; Sih, C. J. *Biocatalysis* **1992**, *6*, 115–126.

(29) Holmquist, M.; Martinelle, M.; Berglund, P.; Clausen I. G.; Patkar, S.; Svendsen, A.; Hult, K. J. *Prot. Chem.* **1993**, *12*, 749–757.

(30) Bianchi, D.; Battistel, E.; Bosetti, A.; Cesti, P.; Fekete, Z. *Tetrahedron: Asymmetry* **1993**, *4*, 777–82.

(31) Zuegg, J.; Honig, H.; Schrag, J. D.; Cygler, M. *J. Mol. Catal. B Enzymol.* **1997**, *3*, 83–98.

(32) Chen, S. T.; Fang, J. M. *J. Org. Chem.* **1997**, *62*, 4349–4357.

(33) We used SWISS-PROT: P25275 for the amino acid sequence of lipase from *Pseudomonas fluorescens*.

(34) Wu, S.-H.; Lai, S.-Y.; Lin, S.-L.; Chu, F.-Y.; Wang, K.-T. *Chirality* **1991**, *3*, 67–70.

(35) Hwang, S. Y.; Brown, K. S.; Gilvarg, C. *Anal. Biochem.* **1988**, *170*, 161–167. Wu, S.-H.; Guo, Z.-W.; Sih, C. J. *J. Am. Chem. Soc.* **1990**, *112*, 1990–1995.

tion), stirring at room temperature for 30 min and desalting (Pharmacia PD-10 column). The protein content of both the acetylated and the deacetylated samples were determined with the Coomassie Blue-binding assay from Bio-Rad using bovine serum albumin as the standard. The degree of acetylation ( $N$ ) was estimated spectrophotometrically using the equation  $N = \Delta\epsilon_{278}M/1160c$ .  $\Delta\epsilon_{278}$  is the change in the extinction coefficient at 278 nm,  $M$  is the molecular weight of the enzyme (33 kDa), 1160 is the difference in the extinction coefficients for *O*-acetyltyrosine and tyrosine, and  $c$  is the protein concentration of the enzyme (mg/mL).<sup>36</sup> We estimate that an average of 10 of the 14 tyrosine residues in PCL were acetylated.

**Nitration of PCL.** Tetranitromethane (300-fold molar excess) was added to a solution of PCL (100 mg in 20 mL in 0.05 M Tris buffer, pH 8 with 5 vol % hexane to promote opening of the lipase lid). After stirring in the dark for various times, a 2.5 mL aliquot was desalted by passing through a gel filtration column (Pharmacia PD-10 column equilibrated with 0.05 M Tris buffer, pH 8). The protein content of the nitrated samples were determined with the Coomassie Blue-binding assay from Bio-Rad using bovine serum albumin as the standard. The degree of nitration was estimated from the increase in extinction coefficient at 275 nm using the equation above. The difference extinction coefficient for 3-nitrotyrosine and tyrosine is 2640 cm<sup>-1</sup> M<sup>-1</sup>. We estimate that an average of 11 of the 14 tyrosine residues in PCL were nitrated.

**Modeling of Transition State Analogues in PCL.** All modeling was done with Discover, version 2.9.7 (Biosym/MSI, San Diego, CA), using the Amber force field except where noted. We used a distance dependent dielectric constant of 4.0 and scaled the 1–4 van der Waals interactions scaled by 50%. The distance dependent dielectric constant damps long-range electrostatic interactions and thus compensates for the lack of explicit solvation.<sup>37</sup> Results were displayed using Insight II, version 95.0 (Biosym/MSI). Protein structures in Figures 3 and 4 were created using RasMac v2.6.<sup>38</sup> Mirosław Cygler and Joseph Schrag of the NRC Biotechnology Research Institute, Montréal, kindly provided the coordinates for PCL. This structure contains a phosphate inhibitor that is not included in the PDB data file (accession code: 3LIP), but is otherwise very similar. Using the Biopolymer module of Insight II, hydrogen atoms were added to correspond to pH 7.0. Histidines were uncharged (singly protonated), aspartates and glutamates were negatively charged, and arginines and lysines were positively charged. The catalytic histidine (His286) was protonated. The inhibitor found in the crystal structure was covalently linked to Ser87. The phosphate inhibitor was first modified to a phosphonate by replacing an oxygen with carbon. Minimization of this structure maintained all five essential

hydrogen bonds. Crystallographic water molecules were included in all minimizations.

Transition state analogues for each alcohol were constructed and manually adjusted to each of the nine staggered local minima possible along bonds b and c. Steric interactions with the enzyme sometimes prevented the starting exactly at the local minimum, but the starting positions were within 15° of the local minima for the free substrate. Energy minimization proceeded in four stages. First, 200 of iterations steepest descent algorithm, all protein atoms constrained with a force constant of 10 kcal mol<sup>-1</sup> Å<sup>-2</sup>; second, 200 iterations of conjugate gradients algorithm with the same constraints; and third, 500 iterations of conjugate gradients algorithm with only the backbone constrained by a 10 kcal mol<sup>-1</sup> Å<sup>-2</sup> force constant. For the fourth stage, minimization was continued using conjugate gradients algorithm without any constraints until the rms deviation reached less than 0.005 Å mol<sup>-1</sup>. Water molecules and the substrate were not constrained through any of the minimization cycles.

**Molecular Dynamics.** Starting from a transition state analogue derived from (*S*)-**1** bound to the active site of PCL, we manually set the torsion angles to -74° and 75° (bonds b and c, respectively, in Table 1). These angles place the phenyl in an unhindered region of the active site. To remove any strong steric repulsions, we minimized the structure first using the steepest descent algorithm (200 iterations, all protein atoms constrained with a force constant of 10 kcal mol<sup>-1</sup> Å<sup>-2</sup>) and then using conjugate gradient algorithm (500 iterations, only protein backbone constrained with a force constant of 10 kcal mol<sup>-1</sup> Å<sup>-2</sup>). We imposed no constraints on the water molecules or substrate during this initial minimization. We ran the molecular dynamics for 1 ps at 300 K for the equilibration period and 25 ps at 300 K for the simulation using a time step of 1 fs with a history file generated every 10 fs. Both torsion angles remained within 20° of their initial settings throughout the simulation. Because this long simulation sampled such a small region of conformational space, we used a systematic search to find the catalytically productive conformations.

**Acknowledgment** is made to the donors of the Petroleum Research Fund, administered by the American Chemical Society, for support of this research. We thank NSERC (Canada) for an equipment grant for the modeling computer and software. We thank Alexandra N. E. Weissfloch for determination of *E* of **2** and determining the absolute configuration, Jessamine Ng for help with the acetylation and nitration of PCL, and Mirosław Cygler and Joseph Schrag (NRC Biotechnology Research Center, Montréal) for access to the X-ray crystallographic coordinates for PCL.

**Supporting Information Available:** Details of the conformational analysis of the free substrates. This material is available free of charge via the Internet at <http://pubs.acs.org>.

JO981783Y

(36) Riordan, J. F.; Vallee, B. L. *Methods Enzymol.* **1967**, *11*, 570–576.

(37) Weiner, S. J.; Kollman, P. A.; Case, D. A.; Singh, U. C.; Ghio, C.; Alagona, G.; Profeta, S., Jr.; Weiner, P. *J. Am. Chem. Soc.* **1984**, *106*, 765–784.

(38) Sayle, R. For information, see <http://www.umass.edu/microbio/rasmol/>.